High-harmonic generation from plasma mirrors at kilohertz repetition rate

Fabien Quéré

High-harmonic generation from plasma mirrors at kilohertz repetition rate

Antonin Borot,[1,*] Arnaud Malvache,[1] Xiaowei Chen,[1] Denis Douillet,[1] Grégory Iaquianiello,[1] Thierry Lefrou,[1] Patrick Audebert,[2] Jean-Paul Geindre,[2] Gérard Mourou,[3] Fabien Quéré,[4] and Rodrigo Lopez-Martens[1]

[1]*Laboratoire d'Optique Appliquée, Ecole Nationale Superieur de Techniques Avancées-Paristech, Ecole Polytechnique, CNRS, 91761 Palaiseau Cedex, France*

[2]*Laboratoire pour l'Utilisation des Lasers Intenses, Ecole Polytechnique, CNRS, 91128 Palaiseau Cedex, France*

[3]*Institut de la Lumière Extrême, Ecole Nationale Superieur de Techniques Avancées-Paristech, Ecole Polytechnique, CNRS, 91761 Palaiseau Cedex, France*

[4]*Service des Photons, Atomes et Molécules, Commissariat à l'Energie Atomique, DSM/IRAMIS, CEN Saclay, 91191 Gif sur Yvette, France*

**Corresponding author: antonin.borot@ensta-paristech.fr*

Received March 3, 2011; accepted March 10, 2011;
posted March 22, 2011 (Doc. ID 142325); published April 14, 2011

We report the first demonstration of high-harmonic generation from plasma mirrors at a 1 kHz repetition rate. Harmonics up to nineteenth order are generated at peak intensities close to 10^{18} W/cm^2 by focusing 1 mJ, 25 fs laser pulses down to 1.7 μm FWHM spot size without any prior wavefront correction onto a moving target. We minimize target surface motion with respect to the laser focus using online interferometry to ensure reproducible interaction conditions for every shot and record data at 1 kHz with unprecedented statistics. This allows us to unambiguously identify coherent wake emission as the main generation mechanism.

OCIS codes: 190.4160, 350.5400.

Femtosecond laser-driven high-harmonic generation (HHG) from plasma mirrors has been earmarked as the next generation, high-brightness attosecond light source [1]. The main experimental objective is to reach the highly efficient relativistic oscillating mirror (ROM) regime [2,3] that operates at laser intensities in excess of 10^{18} W/cm^2 for 800 nm laser light. Because of the high intensities required, most experiments to date have been carried out with terawatt-class peak-power laser systems delivering pulse energies from several tens of milliJoules to several tens of Joules on a single shot basis [4–7]. However, Quéré *et al.* demonstrated another mechanism for HHG in solid density plasmas, coherent wake emission (CWE) [8], operating at intensities as low as a few 10^{15} W/cm^2. This makes it possible to observe HHG from plasma mirrors with driving pulse energies as low as a few milliJoules [8,9] and opens the door to exploring HHG from plasma mirrors using high-repetition-rate lasers.

In this Letter, we present the first demonstration of HHG from plasma mirrors driven at a kilohertz repetition rate. The experiment was performed using the "Salle Noire" laser system at the Laboratoire d'Optique Appliquée, which routinely delivers 2.5 mJ, 25 fs pulses generated by a commercial 1 kHz Ti:sapphire chirped-pulse amplifier front end from Femtolasers GmbH (Femtopower Compact Pro CE Phase) followed by a homemade booster amplifier [10]. Before entering the interaction chamber, the laser beam is spatially filtered under vacuum through a 1-m-long hollow waveguide with a 250 μm core diameter. Then, the remaining 1 mJ beam is focused onto a moving target by an $f/1.7$, silver-coated, 25° off-axis parabola down to a spot size of 1.7 μm FWHM without wavefront correction. The maximum peak intensity on target is approximately 10^{18} W/cm^2. Under these conditions, the temporal contrast of the laser ($>10^7:1$) is sufficient to avoid target preionization by amplified spontaneous emission or prepulses before the arrival of the pulse peak.

The experimental setup is shown in Fig. 1. The beam reflected off the target is then sent onto a 600 grooves/mm, gold coated, aberration-corrected, flat-field, grazing incidence spherical diffraction grating with a 10% to 30% efficiency in the 125 to 22 nm wavelength range. The diffracted harmonic spectrum is detected using a single stage multichannel plate (MCP) coupled to a phosphor screen imaged onto a high-dynamic-range (12 bit) CCD camera. The MCP and imaging system are mechanically translated along the spectrometer image plane to record full harmonic spectra. Precautions are taken to avoid any stray emission (laser light or particles) onto the MCP from the plasma-generated on target; in this way, no filter is needed. The combination of a very small point source emission (<2 μm) and the use of an aberration-corrected grating as well as a single stage MCP yields a measured resolution (using known plasma emission lines) better than 0.2 nm over the full spectral range.

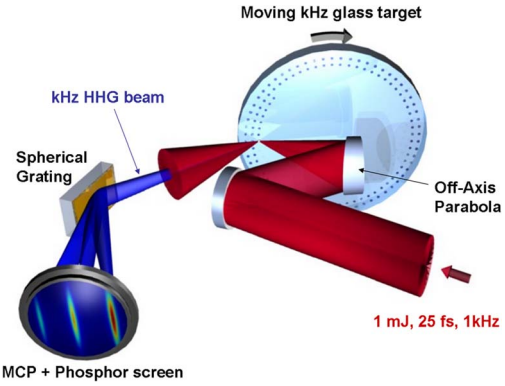

Fig. 1. (Color online) Experimental setup for plasma mirror HHG at 1 kHz.

Laser–solid target interaction at high repetition rate is far from trivial as the target surface needs to be quickly refreshed between each shot while maintaining identical interaction conditions. Doing so with milliJoule energy pulses demands that the target surface be positioned with respect to the laser focus with a precision better than the Rayleigh length typically of the order of a few micrometers (8.2 μm in our case). The use of a nonimaging spectrometer with a centimeter-size detector placed about a meter away from the HHG source also means keeping the angle between the target normal and the direction of laser propagation in the few hundred microrad range to avoid spreading of the signal in the vertical direction on the detector when averaging over multiple shots. Lastly, because of rapid consumption of the target at high repetition rates, large surface area targets moving at several centimeters per second must be used to accumulate a significantly large number of shots before changing the target. Our target consists of a 14 cm diameter circular BK7 glass substrate mounted on a rotating and translating holder. It is rotated over a full period after which it is translated and rotated again in order to draw a shot pattern concentric with the previous one. Repeated across the whole target surface and imposing a 100 μm distance between each shot to avoid debris from previous shots, this procedure allows us to achieve up to 1.5 million consecutive shots per target face at 1 kHz.

We use an online optical technique to probe and minimize target motion during experiments. We set up a Mach–Zehnder interferometer with a frequency-stabilized He–Ne laser (for better fringe stability and longer coherence length), where one arm is reflected off the moving target and another off a fixed mirror. The spatial fringe pattern generated by the recombination of the two arms of the interferometer is recorded online with a CCD camera. From the fringe displacement, we deduce the real-time changes in target surface position (i.e., the horizontal displacement) and angle of orientation (i.e., the two coordinates of the vector normal to the target surface). A set of two picomotor actuators are then used to minimize the precession of the target normal with respect to the rotation axis. Operational target stability measurements are presented in Fig. 2. Residual target surface motion is 1.7 μm peak-to-valley in position (310 nm standard deviation) and 80 μrad peak-to-valley in orientation (25 μrad standard deviation), which, in this case, is amply sufficient for continuous operation at 1 kHz.

Figure 3(a) shows a typical harmonic spectrum averaged over 100 consecutive shots (corresponding to a 100 ms camera exposure time) at a peak intensity of 8×10^{17} W/cm^2. We observe narrow and well-contrasted peaks corresponding to harmonic orders 7 to 19. The observed lower amplitude of harmonic order 7 is due to the bottom edge of the MCP spectral response. Because our spectrometer is nonimaging, the spectrum shown is integrated over a central portion of the harmonic beam [Fig. 3(b)] spanning 10 mrad of the 20–30 mrad FWHM average divergence angle around harmonic 13 and thus does not take into account the respective divergences of the individual harmonics. To estimate the correct laser-to-harmonics conversion efficiency, each harmonic line is integrated angularly (vertical direction) and spectrally (horizontal direction) and their respective energies are then estimated by computing the "transfer functions" of each component of our spectrometer for each harmonic order: the efficiency of the grating, the quantum efficiency of the photon-to-electron conversion of the MCP, the MCP gain, the electron-to-photon conversion of the phosphor screen, the collection efficiency of the imaging system as well as the response of the CCD camera. We finally estimate the overall conversion efficiency for all harmonics from 9 to 17 to be higher than 3×10^{-6}. Estimated generation efficiencies per harmonic are presented in Fig. 3(c).

Several observations lead us to conclude that the harmonics observed are generated via the CWE mechanism rather than via the ROM mechanism. First, our peak intensity on target lies below the relativistic limit for 800 nm light, which corresponds to the onset of ROM. Second, the highest harmonic order observed (19) is very close to the maximum plasma frequency of fully ionized silica at the initial solid density, which indeed corresponds to the expected plasma conditions with our interaction parameters. This is consistent with CWE emission. Finally, to support this conclusion, we measured the

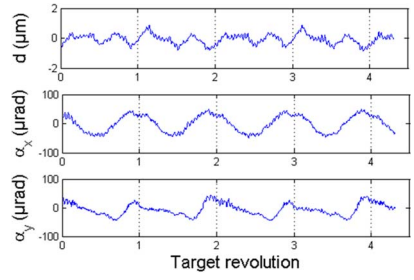

Fig. 2. (Color online) (a) Position, (b) tangential, and (c) azimuthal angle variations measured over four full target revolutions [11].

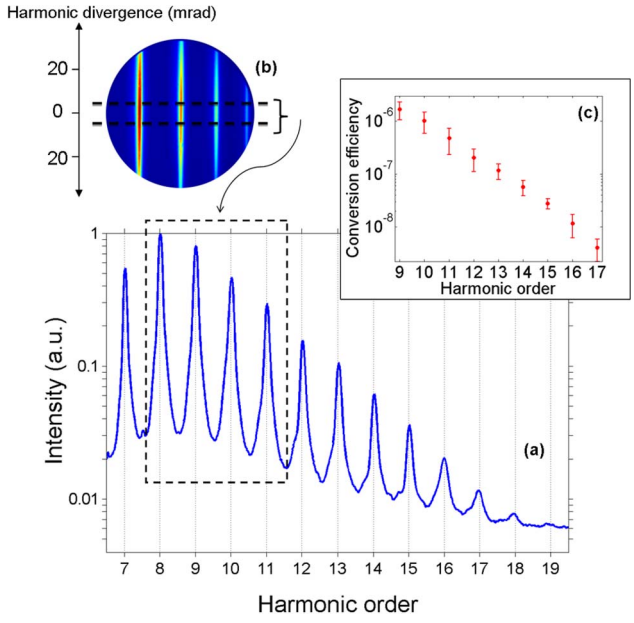

Fig. 3. (Color online) (a) Typical harmonic spectrum averaged over 100 shots and integrated over the (b) central part of the HHG beam. (c) Estimated conversion efficiency for harmonic 9 to 17.

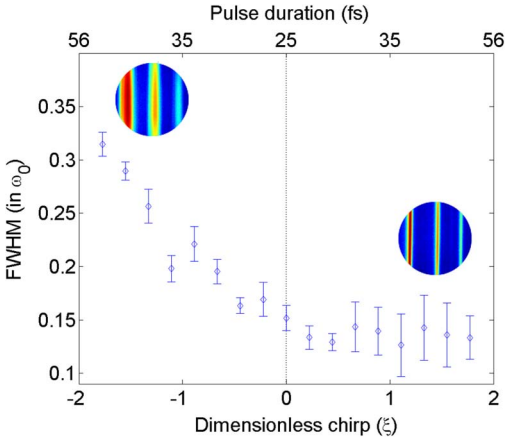

Fig. 4. (Color online) Evolution of spectral width of harmonic 8 with driving laser chirp (ω_0 is the central angular frequency of the laser).

dependence of the harmonic spectral widths on the chirp of the driving laser, which is characteristic of sublaser cycle dynamics of the CWE process [12]. This dependence manifests itself experimentally by either a broadening or a narrowing of the individual harmonic peaks for a respectively negative or positive input laser chirp. This behavior is exactly reproduced in our experiment, as illustrated in Fig. 4, which shows the measured change in spectral width for harmonic order 8 as a function of the dimensionless laser chirp (ξ) and concomitant laser pulse duration $\tau = \tau_0\sqrt{1+\xi^2}$, where τ_0 is the Fourier transform-limited pulse duration.

In conclusion, we demonstrate kilohertz-driven HHG from plasma mirrors for the first time. High on-target intensities can be achieved using tightly focused milliJoule energy pulses without deformable mirror wavefront correction simply by spatially filtering the laser beam through a hollow waveguide prior to focusing. CWE is clearly identified as the main mechanism responsible for HHG. By filling the hollow waveguide with a rare gas for spectral broadening and using chirped mirrors for temporal compression, our laser system can be modified to generate highly focusable milliJoule energy few-cycle pulses featuring full carrier-envelope control [13]. This should allow us to guide the HHG process with sublaser cycle precision.

Financial support from the CNRC-CNRS 2007 program and the Agence Nationale pour la Recherche, through programs Chaire d'Excellence 2004, Blanc 2006 (ILAR) and Jeunes Chercheuses et Jeunes Chercheurs 2009 (UBICUIL), as well as the European Research Council (grant agreement 240013) are gratefully acknowledged.

References and Note

1. G. Tsakiris, K. Eidmann, J. M. ter Vehn, and F. Krausz, New J. Phys. **8** (2006).
2. R. Lichters, J. Meyer-Ter-Vehn, and A. Pukhov, Phys. Plasmas **3**, 3425 (1996).
3. S. V. Bulanov, N. Naumova, and F. Pegoraro, Phys. Plasmas **1**, 745 (1994).
4. A. Tarasevitch, K. Lobov, C. Wünsche, and D. von der Linde, Phys. Rev. Lett. **98**, 103902 (2007).
5. C. Thaury, F. Quere, J.-P. Geindre, A. Levy, T. Ceccotti, P. Monot, M. Bougeard, F. Reau, P. d'Oliveira, P. Audebert, R. Marjoribanks, and P. Martin, Nat. Phys. **3**, 424 (2007).
6. B. Dromey, M. Zepf, A. Gopal, K. Lancaster, M. S. Wei, K. Krushelnick, M. Tatarakis, N. Vakakis, S. Moustaizis, R. Kodama, M. Tampo, C. Stoeckl, R. Clarke, H. Habara, D. Neely, S. Karsch, and P. Norreys, Nat. Phys. **2**, 456 (2006).
7. Y. Nomura, R. Horlein, P. Tzallas, B. Dromey, S. Rykovanov, Z. Major, J. Osterhoff, S. Karsch, L. Veisz, M. Zepf, D. Charalambidis, F. Krausz, and G. D. Tsakiris, Nat. Phys. **5**, 124 (2009).
8. F. Quere, C. Thaury, P. Monot, S. Dobosz, P. Martin, J.-P. Geindre, and P. Audebert, Phys. Rev. Lett. **96**, 125004 (2006).
9. J. H. Easter, A. G. Mordovanakis, B. Hou, A. G. R. Thomas, J. A. Nees, G. Mourou, and K. Krushelnick, Opt. Lett. **35**, 3186 (2010).
10. L. Canova, X. Chen, A. Trisorio, A. Jullien, A. Assion, G. Tempea, N. Forget, T. Oksenhendler, and R. Lopez-Martens, Opt. Lett. **34**, 1333 (2009).
11. The double periodicity in position and orientation comes from the fact that the cylindrical ball bearings inside the rotation stage require two target revolutions to fully rotate themselves. We observe here ball-bearing defaults.
12. F. Quere, C. Thaury, J.-P. Geindre, G. Bonnaud, P. Monot, and P. Martin, Phys. Rev. Lett. **100**, 095004 (2008).
13. X. Chen, A. Malvache, A. Ricci, A. Jullien, and R. Lopez-Martens, Laser Phys. **21**, 198 (2011).